Structure Design and Driving Dynamics Research of Crane Wheel Fatigue Test Device

Jingjie Yuan*, Lei Zhang[a], Haijun Jia[b], Dugang Kang[c], Shangyuan Jia[d], Shuihong Yi[e]

Chongqing Special Equipment Inspection and Research Institute, Chongqing, China

Key Laboratory of Electromechanical Equipment Security in Western Complex Environment for State Market Regulation, Chongqing, China

* Corresponding Author Email: scu_yuan@qq.com, [a]zl_816@163.com, [b]851497645@qq.com, [c]173191588@qq.com, [d]1458018035@qq.com, [e]Yishuihong12367@126.com

Abstract. In order to explore the fatigue damage of the crane wheel, the contact stress between the crane wheel and the steel rail was calculated. Moreover, the fatigue mechanism of crane wheels was also discussed by deriving the theoretical wheel pressure formula. As a result, a device design idea based on the fatigue mechanism of the crane wheel was proposed, where the device can be used to detect the bearing capacity, wear resistance and fatigue resistance of crane wheels. By using the simulation methods, the structure requirements and driving dynamics of the test device for different wheel diameters and wheel pressures were investigated and validated. Finally, the structural diagram of the fatigue test device is presented to provide the design guidance for the experiment research of the fatigue properties and reliability of crane wheels.

Keywords: fatigue damage, crane wheel, fatigue mechanism, device design, driving dynamics, structural design

1. Introduction

The cranes play a very important role in industrial production. They can transport materials from one place to another and realize the trans-regional transfer of materials. As one of the key components of the crane, the crane wheels are primarily used to support the load and to implement the function of the crane running back and forth over the track. Due to the presence of alternating stresses, the crane wheels will constantly suffer from the fatigue damage during crane operations. This fatigue damage can cause the surface of the wheel to detach and develop imperceptible cracks, which greatly reduces the service life of crane wheels and seriously threatens the safe operation of the crane. Therefore, it is of great importance to study the fatigue properties and reliability of crane wheels in order to ensure the performance and safety of the crane.

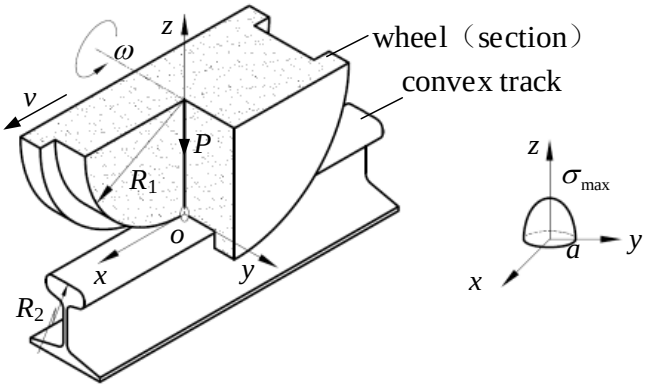
In fact, some related investigations on this field have been accomplished. As a result, Zhou Zhiao [1] and Ren Tao [2] investigated the the fatigue mechanism of the wheel-rail tread of the crane. Wang Fuyuan [3] proposed a calculation model for the wear of the crane wheel rim by analyzing the theoretical lateral forces and discussing the relationship between the lateral forces and the wear. Wu Fengqi et al. [4] established a crane fatigue life model based on the wheel load test using the virtual prototype technology and explained the inspection mechanism.

However, unfortunately, these aforementioned studies mainly investigate the damage mechanisms and do not synthetically focus on the test techniques for the fatigue properties and reliability of crane wheels. It seems that the relevant test data on the fatigue properties and reliability are insufficient to support the design and selection of crane wheels. Especially, there is still a lack of the comprehensive testing device to detect the bearing capacity, wear resistance and fatigue resistance of crane wheels.

Based on these facts, it is essential to further develop the testing techniques for the fatigue properties and reliability of crane wheels. This work, thus, aims to focus on the development of the wheel fatigue test device. The fatigue mechanism of the crane wheels was stressed. The design and driving dynamics of the device were discussed and studied in detail.

2. Fatigue Mechanism

As shown in Fig. 1, the crane wheels are squeezed and contacted with the top of the rail under the action of wheel loads. Ideally, a wheel with cylindrical tread will have line contact with a flat track, and a wheel with conical (or cylindrical) tread will have point contact with a raised track. The point contact is taken as an example for analysis below. It shows the situation when the cylindrical tread wheel is in contact with the convex track. From the physical model, it is a point contact, but the contact spot is actually a circle with a radius a located in the x-o-y plane, as shown in Fig. 1(b), the contact stress is distributed along the arc of the semi-ellipsoid, reaching the maximum in the z-direction of the wheel, and the contact stress at the edge point is zero.



(a) model with point contact (b) contact stress distribution

Figure 1. Model with point contact based on Hertz theory

According to Hertz theory, the contact stress at any point in the semi-ellipsoid can be expressed as follows [5]:

$$\sigma = \sigma_{\max}\sqrt{1-\left(\frac{r}{a}\right)^2}$$

Where $\sigma_{\max}$ is the maximum value of the contact stress, r is one of radius within contact circle, a is radius of contact circle, and

$$a = \left(\frac{3PR_1R_2}{4\bar{E}(R_1+R_2)}\right)^{1/3}$$

Where P is wheel load exerted by lifting objects; R_1 and R_2 are arc radius of the two contact bodies; $\bar{E}$ is the equivalent modulus of elasticity, and

$$\bar{E} = 1/\left(\frac{1-\mu_1^2}{E_1}+\frac{1-\mu_2^2}{E_2}\right)$$

Where μ_1 and μ_2 are arc the poisson's ratio of two contact bodies material.

According to Newton's third law of motion,

$$P = \iint_s \sigma dxdy = \iint_s \sigma_{\max}\sqrt{1-\left(\frac{r}{a}\right)^2}dxdy = \frac{2\pi a^2\sigma_{\max}}{3}$$

That is,

$$\sigma_{\max} = \frac{3P}{2\pi a^2} \tag{1}$$

Substituting the expression of a into formula (1), we have obtain

$$\sigma_{\max} = 0.5784P^{1/3}\left(\frac{R_1R_2}{\bar{E}(R_1+R_2)}\right)^{-2/3} \tag{2}$$

Equation (2) shows that the maximum contact stress of the crane wheel is related to the wheel pressure, the material and structural parameters of the wheel and wheel rail. After the material and structure of the wheel and wheel rail are determined, the maximum contact stress is only related to the wheel pressure.

During the operation of the crane, the wheel moves along the x-o axis and rotates about its own symmetry axis in the x-o-z plane. Obviously, the stress at a certain point in contact with the wheel rail will change periodically according to the curve shown in Fig. 2, that is, the amplitude of the load P does not change in contact location,but the contact point position is periodically constant with time. This brings fatigue damage to the wheel, and in severe cases, the wheel will crack or even collapse [6]. Therefore, the load of the crane, that is, the contact stress brought by the wheel pressure must be lower than the fatigue strength value of the crane wheel within the fatigue life, and the fatigue strength value of the wheel is mainly obtained through software simulation and experimental testing.

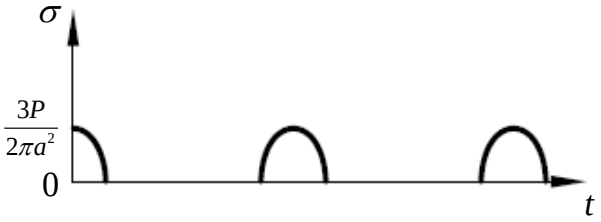
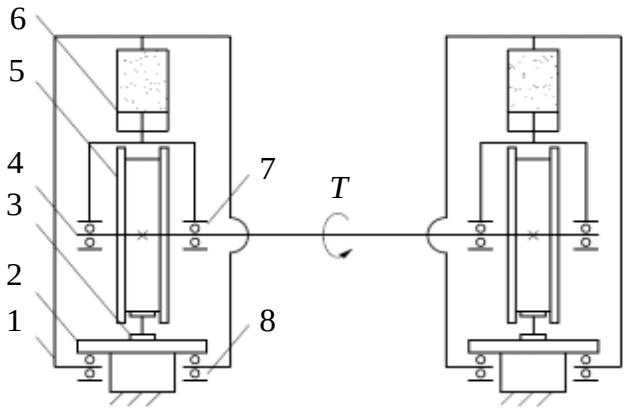


Figure 2. Stress-time curve of a certain point on the wheel

3. Design ideas

In order to study the relationship between crane wheel fatigue wear and wheel pressure, the design scheme of the crane wheel fatigue test device is proposed as shown in Fig. 3. The device is mainly composed of wheels, tracks, main shaft, frame, rods and oil cylinder. The wheels which are fixed with main shaft are arranged on the main shaft, and the rest of the components are symmetrically arranged.



1-rod；2-frame；3-track；4-main shaft；5-wheel；
6-cylinder；7-main bearing；8-load bearing

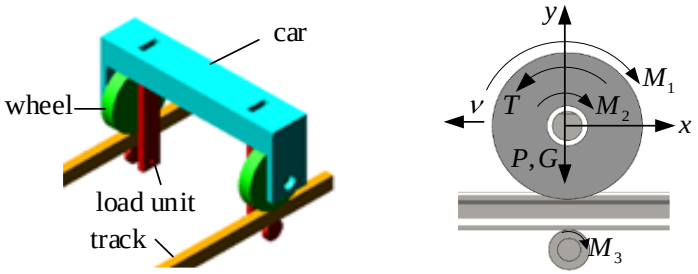
Figure 3. Design scheme of wheel fatigue test device

The wheel walking power is input by main shaft, and the main shaft drives the wheels at both ends to rotate synchronously. The wheel load of the wheel is provided by the oil cylinder, the oil cylinder piston rod is connected with the main shaft through the main bearing, and the oil cylinder block transmits the load which is coming from the oil cylinder to the frame through the wheel load bearing through the connecting rods. According to the theorem of action force and reaction force, the oil cylinder provides the wheel load of the crane wheel. By changing the pressure of the liquid in the inner cavity of the oil cylinder, the load required for the fatigue life test can be applied to the wheel.

4. Driving dynamics research

4.1. Dynamics Model

Taking the crane wheel with a diameter of 500 mm as an example, the wheel fatigue test device should be designed to conform to the fatigue test requirements of crane wheels, where the maximum wheel pressure of a wheel with a diameter of 500 mm is 600 kN according to the crane design code [7]. Based on these technical data, the dynamic model of the test device shown in Fig. 4(a) was constructed, and the corresponding force diagram was expressed in Fig. 4(b).



(a) 3-D model (b) Force Analysis Diagram

Figure 4. Dynamic model of wheel fatigue test device

4.2. Walking Torque Calculation

According to the knowledge of mechanics, the following formulas can be found:

$$T = T_1 + T_2$$

$$T_1 - (M_1 + M_2 + M_3 + M_4 + M_5) = 0 \tag{3}$$

$$T_2 - T_1 = J\beta \tag{4}$$

$$M_1 = \delta(P+G)$$
$$M_2 = \mu d_1 (P+G)$$
$$M_3 = \mu P d_2$$
$$M_4 = \frac{1}{2} d_0 G \tan\alpha$$
$$M_5 = \frac{1}{2} CpAd_0$$

Where T is drive torque; T_1 is drive torque in uniform speed mode; T_2 is drive torque in acceleration or deceleration mode; M_1 is wheel rolling torque; M_2 is friction torque of main bearing; M_3 is friction torque of load bearing; M_4 is additional torque in inclined walking mode; M_5 is additional torque supported by wind load; J is equivalent moment of inertia of car; β is wheel angular acceleration.

Substituting the expressions of M_1, M_2, M_3, M_4 and M_5 into (3), we have obtain the drive torque in uniform speed mode:

$$T_1 = k\left[\delta(P+G) + \mu d_1 (P+G) + \mu P d_2\right] + \frac{1}{2} d_0 G \tan\alpha + \frac{1}{2} CpAd_0 = 1529.6\,\mathrm{N\cdot m} \tag{5}$$

Where δ is coefficient of rolling friction, $\delta = 0.0005\,\mathrm{m}$; G is the weight of car, $G = 2\times10^4\,\mathrm{N}$; P is load exerted by lifting objects, $P = 6\times10^5\,\mathrm{N}$; μ is coefficient of rolling friction of bearing, $\mu = 0.004$; d_0 is diameter of wheel, $d_0 = 0.5\,\mathrm{m}$; d_1 is diameter of main shaft, $d_1 = 0.1\,\mathrm{m}$; d_2 is diameter of load shaft, $d_2 = 0.07\,\mathrm{m}$; α is incline angle of tracks, $\alpha = 1/1500$; k is additional

coefficient brought by the frictional resistance between the wheel rim and the track and the drag torque coefficient caused by accessories such as cables, etc. $k=1.2$; C is coefficient of wind load, $C=1.2$; p is wind equivalent pressure, $p=240\,\mathrm{N/mm^2}$; A is the frontal pressure area, $A=2.5\mathrm{m^2}$.

Substituting the expressions of $J=J_1+J_2+\frac{Gd_0^2}{4g}$ and $\beta=\frac{2\alpha}{d_0}=\frac{2}{d_0}\frac{dv}{dt}$ into (4), we have obtain the drive torque in acceleration mode:

$$T_2=T_1+\frac{2}{d_0}\left(J_1+J_2+\frac{GD^2}{4g}\right)\frac{dv}{dt}=1982.8\mathrm{Nm} \tag{6}$$

Where J_1 is moment of inertia of wheel, $J_1=8.231\mathrm{kg\cdot m^2}$; J_2 is moment of main shaft, $J_2=0.085\mathrm{kg\cdot m^2}$; g is acceleration of gravity, $g=9.8\mathrm{m/s^2}$; v is velocity of car, $v=1.2\,\mathrm{m/s}$; t is acceleration time of car, $t=1.5\mathrm{s}$.

4.3. Walking Power Calculation

When the car travels at a constant speed, according to the power definition:

$$P_1=\frac{T_1\times n}{9550}=\frac{1529.6\times 45.84}{9550}=7.34\mathrm{kW} \tag{7}$$

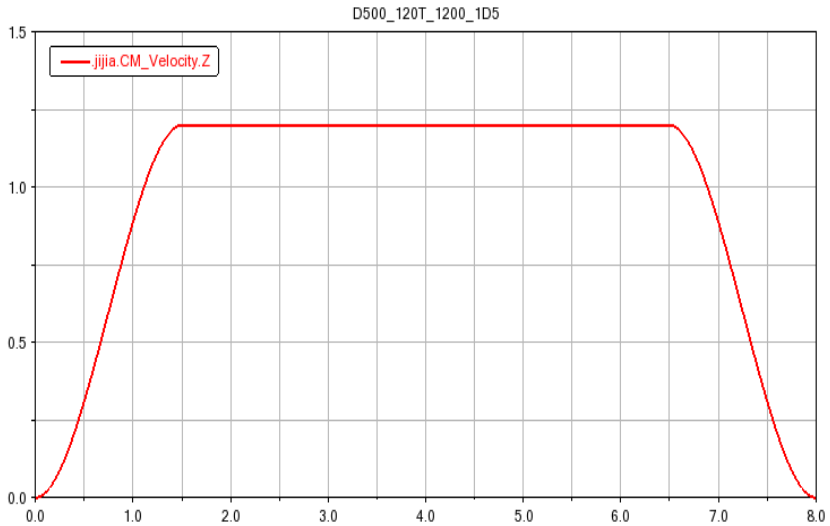
Where P_1 is walking power in constant speed mode; T_1 is drive torque in uniform speed mode, and $T_1=1529.6\ \mathrm{N\cdot m}$ according to (5); n is rotating speed of wheel, $n=(60v)/(\pi d_0)=45.84\,\mathrm{rpm}$.

When the car starts from rest, according to the power definition:

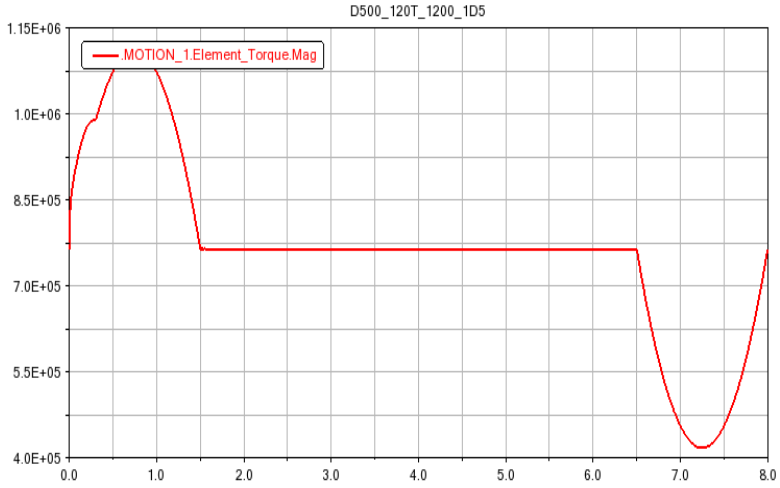
$$P_2=\frac{T_2\times n}{9550}=\frac{1982.8\times 45.84}{9550\times 2}=9.52\mathrm{kW} \tag{8}$$

4.4. Dynamics Software Simulation

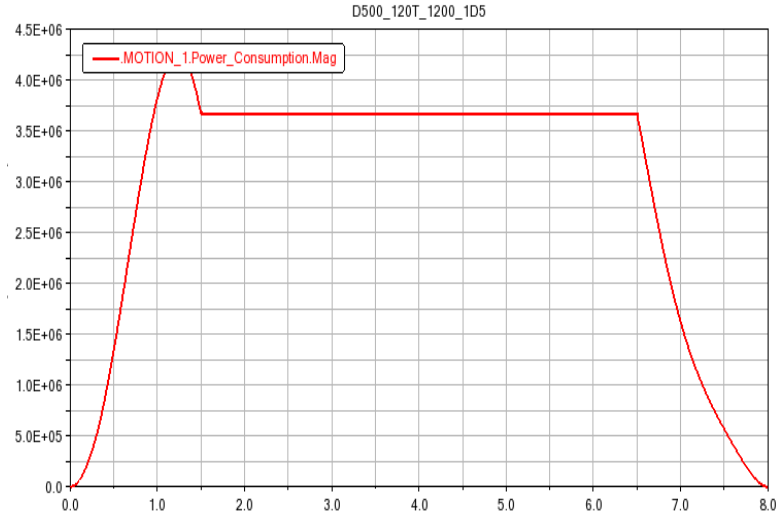
The dynamic simulation of the model was carried out. It is found that the wheel with a diameter of 500 mm is walking as shown in Fig. 5 under the working conditions of 120 tons of wheel load, 1.2 m/s speed, and 1.5 s acceleration time. The speed curve, the driving torque curve of a single wheel and the power curve of a single wheel are, respectively, shown in Fig. 5(a), Fig. 5(b) and Fig. 5(c).



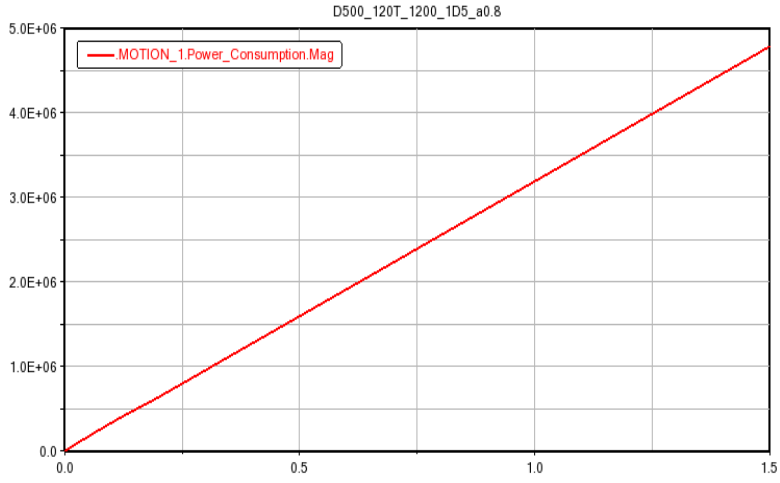
(a) Speed-time curve



(b) Torque-time curve



(c) Power-time curve



(d) Power-time curve

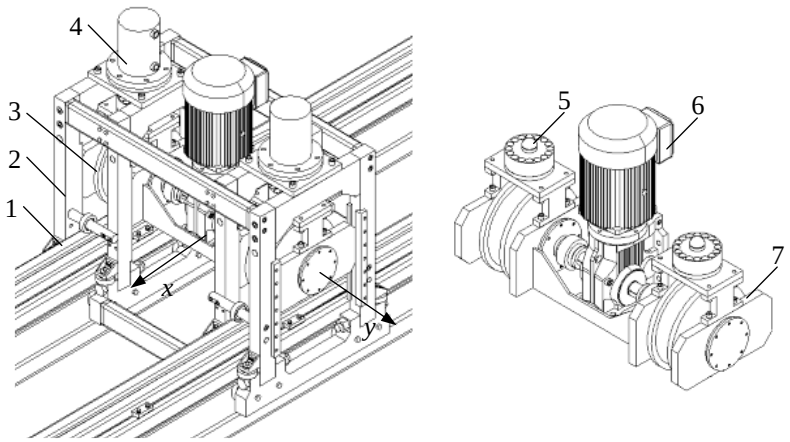
Figure 5. Dynamic simulation of wheel fatigue test device

The driving torque (764.8 N·m) shown in Fig. 5(b) is consistent with half of the torque value calculated by (5), but the peak value of torque (1112.2 N·m) calculated by simulation is higher than that of (6) is slightly larger than half of the calculated moment value because the angular acceleration set by the STEP function is used in the simulation, and its curve is not uniform acceleration. The driving power (3.67 kW) shown in Fig. 5(c) is consistent with half of the value calculated by (7), but

the peak power (4.25 kW) calculated by simulation is higher than that calculated by (8).The calculated power value is relatively small, because the maximum speed is used in the calculation of (8), and the average speed should be used in theory. If the uniform acceleration condition is adopted, as shown in Fig. 5(d), the power peak (4.79 kW) calculated by the simulation is close to the power value calculated by (8), because the power is proportional to the speed, the speed reaches the maximum at the end, so its power will also reach the maximum. However, in practice, the factors such as mechanical power and motor power need to be considered, and a safety factor greater than 1 needs to be introduced.

5. Structural design

The structural design diagram of the wheel fatigue test device is presented in Figure 6. It can be seen that the fatigue test device is mainly composed of a track assembly, a car assembly, a driving wheel assembly and an oil cylinder assembly, etc.. The traveling power of the car is supported by both ends of the motor.



1-track；2-car；3-wheel；4-oil cylinder；
5-sensor；6-motor；7-slider

Figure 6. Structural design diagram of the wheel fatigue test device

During testing, the car travels back and forth along the track assembly, that is, along the x-direction, and the wheel pressure is transmitted from the oil cylinder to the force sensor and then applied to the wheel drive shaft. When replacing the wheel, the wheel can be removed and replaced along the y-direction. The drive shafts and guide rails used in the test are different for the crane wheels with different diameters and can be selected by searching the standard rules. In general, wheels with diameters of 400 mm and 200 mm recommend the P43 and P12 guide rails, respectively.

6. Conclusion

To further deepen the understanding of fatigue damage, theoretical analysis has been performed to discuss the fatigue mechanism of crane wheels. The design schemes have been proposed for the fatigue test device, which can be used to detect the bearing capacity, wear resistance and fatigue resistance of crane wheels. The structure and driving dynamics of the test device have been studied and validated by using the simulation methods. Finally, the structural diagram of the fatigue test device is presented to provide the design guidance for the experiment research of the fatigue properties and reliability of crane wheels.

Acknowledgments

This work was financially supported by Chongqing Technology Innovation and Application Development Project (No. cstc2019jscx-msxmX0065).

References

[1] Z. Zhou, “Fatigue calculation of crane wheel tread,” Hoisting and Conveying Machinery, China, vol.1, pp.8-11, January 1993.

[2] T. Ren, “Wheel mechanism and life analysis of wheel-rail tread of crane,” Taiyuan University of Science and Technology, 2021.

[3] F. Wang, “Theoretical analysis of deflection lateral force and prediction of wheel wear for bridge Crane,” Taiyuan University of Science and Technology, 2020.

[4] F. Wu, X. Tang, Z. Yu, E. Liu, H. Xiu, “Research on wheel pressure of crane based on experimental test and finite element analysis,” Hoisting and Conveying Machinery, China, vol.11, pp.53-55, November 2011.

[5] J. Halling, Principles of Tribology, The Macmillan Press LTD,1975.

[6] H. Liu, Mechanics of Materials II, 6rd ed., Beijing: Higher Education Press, 2017.

[7] GB/T 3811-2008, Design code for crane, Beijing: China Standard Press, 2008.